Thermal Analysis of Steel Blade Quenching by Induction Heating

Yoshihiro Kawase, *Member, IEEE*, Tsutomu Miyatake, and Katsuhiro Hirata, *Member, IEEE*

***Abstract*—This paper introduces a computational method for predicting the temperature characteristics of steel quenching by induction heating. In this method, an eddy current analysis is coupled with a thermal analysis using the 3-D finite element method. The nonlinear characteristics of the electric conductivity of steel is taken into account. The validity of this method is confirmed through the comparison with measured results when applied to a steel blade quenching of an electric shaver.**

***Index Terms*—Eddy current, induction heating, thermal analysis.**

I. Introduction

THERE are some kinds of instant quenching methods; the electric heating by high power voltage source, the induction heating by high frequency power source, and so on. The induction heating equipment, which generates an eddy current in the conductor by high frequency current, is thought to be suitable for the use of local heating. Then, this method is adopted so that the steel blade of a shaver can be locally and uniformly quenched because the hardness of the steel is greatly influenced by heating conditions.

It is very important to obtain the optimal specification and conditions of the heating equipment by the analytical approach, authors have been studying the coupled problem of the magnetic analysis and the thermal analysis [1].

In this paper, nonlinear characteristics of the electric conductivity of steel blade is taken into account when partially heated up to about 1000°C. The effectiveness of this method is clarified though the comparison with the measured results when applied to obtain the temperature distribution of the steel blade of a shaver by induction heating quenching. Furthermore, the influences of the ferrite cores and the coil shapes on the magnetic flux, eddy current and temperature distributions of the steel blade are clarified.

II. Analysis Method

A. Current Vector Analysis

A model with complex shape makes it difficult to precisely analyze the distribution of the current vector in the finite element analysis. Therefore, the current density vector [2], [3] for each element should be computed beforehand using (1)

$$\mathrm{rot}\left(\frac{1}{\sigma}\mathrm{rot}\boldsymbol{T}\right)=0,\quad \boldsymbol{J}_0=\mathrm{rot}\boldsymbol{T} \tag{1}$$

Here, σ is conductivity, $\boldsymbol{T}$ is current vector potential, and $\boldsymbol{J}_0$ is current density.

B. Eddy Current Analysis

In the next step, eddy current analysis is carried out using (2) to obtain the Joule loss.

$$\mathrm{rot}\left(\frac{1}{\mu}\mathrm{rot}\boldsymbol{A}\right)=\boldsymbol{J}_0+\boldsymbol{J}_\mathrm{e},\quad \boldsymbol{J}_\mathrm{e}=-\sigma\left(\frac{\partial \boldsymbol{A}}{\partial t}+\mathrm{grad}\phi\right) \tag{2}$$

Here, μ is permeability, $\boldsymbol{A}$ is the magnetic vector potential, $\boldsymbol{J}_0$ is the current density obtained by (1), $\boldsymbol{J}_\mathrm{e}$ is the eddy current density, and ϕ is the electric scaler potential.

C. Transient Thermal Analysis

Transient thermal analysis is carried out using Joule loss density above obtained as a heat source. The fundamental equation of thermal analysis is as follows,

$$\frac{\partial}{\partial x}\left(K_{xx}\frac{\partial\theta}{\partial x}\right)+\frac{\partial}{\partial y}\left(K_{yy}\frac{\partial\theta}{\partial y}\right)+\frac{\partial}{\partial z}\left(K_{zz}\frac{\partial\theta}{\partial z}\right)+Q=dc\frac{\partial\theta}{\partial t} \tag{3}$$

Here, θ is the temperature, K_{xx}, K_{yy}, and K_{zz} are the thermal conductivities in x, y, and z directions, respectively, d is the material density, and c is the specific heat. Q is the Joule loss obtained by the equation (4).

$$Q=\frac{\boldsymbol{J}^2}{\sigma}=\frac{(\boldsymbol{J}_0+\boldsymbol{J}_\mathrm{e})^2}{\sigma} \tag{4}$$

In this analysis, the nonlinear characteristic of the electric conductivity is taken into account so that the CPU time can be saved as follows.

Some patterns of Joule loss according to the electric conductivity are beforehand prepared, and this value is changed by linear interpolating approximation using these patterns.

The electric conductivity σ_θ at temperature θ taking into account the temperature rise is derived from the following equation.

$$\frac{1}{\sigma_\theta}=\rho_{20}\left(1+\alpha_{20}\theta_r\right) \tag{5}$$

Here, θ_r is the temperature rise, ρ_{20} and α_{20} are the electrical resistivity and the temperature coefficient at 20°C, respectively.

III. Analyzed Model

Fig. 1 shows the analyzed model used in this study. The steel blade of this model has 28 convex parts (27 concave slits). The

Manuscript received October 25, 1999.

Y. Kawase and T. Miyatake are with the Department of Information Science, Gifu University (e-mail:{ kawase; miya}@info.gifu-u.ac.jp).

K. Hirata is with the Analytical Technology Research Laboratory, Matsushita Electric Works, Ltd. (e-mail: hirata@ertc.mew.co.jp).

Publisher Item Identifier S 0018-9464(00)06731-5.

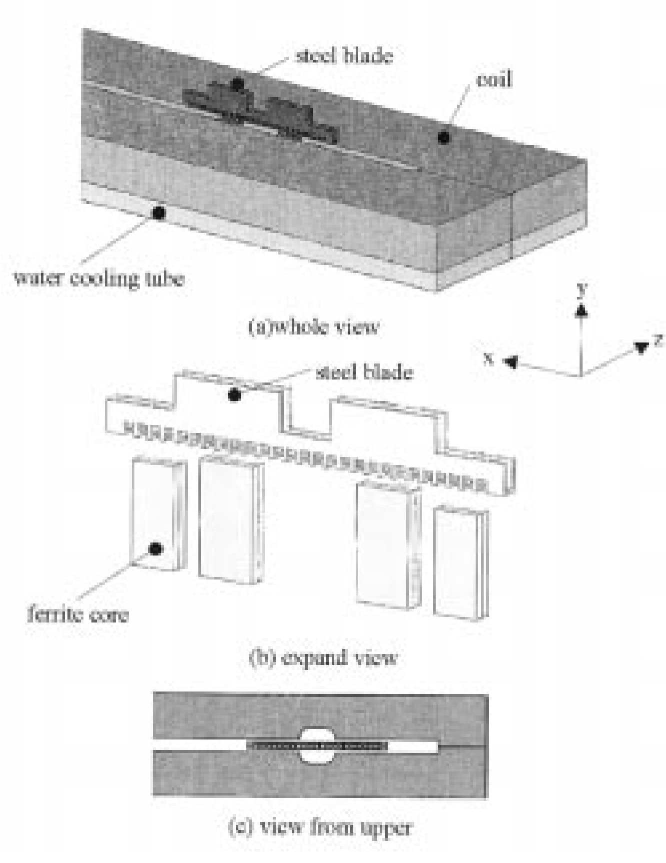

Fig. 1. Analyzed model.

TABLE I
PROPERTIES OF CONSISTING MATERIALS

Part	Electric Conductivity (S/m)	Thermal Conductivity (W/m°C)	Specific Heat (J/kg°C)	Density (kg/m^3)
steel blade	1.82×10^7	19	470	7860
ferrite core	1.00×10^3	1.5	1070	2300
coil	1.55×10^7	1.5	430	8930

quenching equipment has four ferrite cores set under the blade so that the magnetic flux can be concentrated on the tips of the blade and the eddy current efficiently can flow in the blade. One turn coil made of copper have a copper tube for water cooling. The input supply is a sinusoidal voltage of 293 V with a frequency of 348 kHz. The electric conductivity, the thermal conductivity, specific heat, and material density of each part are showed in Table I. The heat transfer and the room temperature is assumed to be 30 $W/m^2\cdot°C$ and 25°C, respectively.

IV. Results and Discussion

A. Comparison with Measured Results

Fig. 2 shows how temperature changes over time with actual measured values. Both results have a good agreement as shown

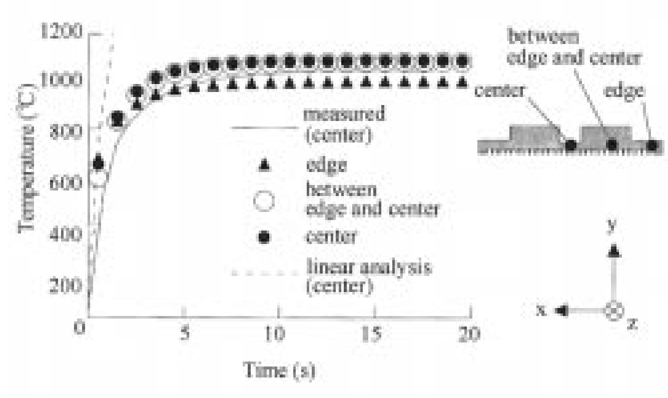

Fig. 2. Time variations of temperature.

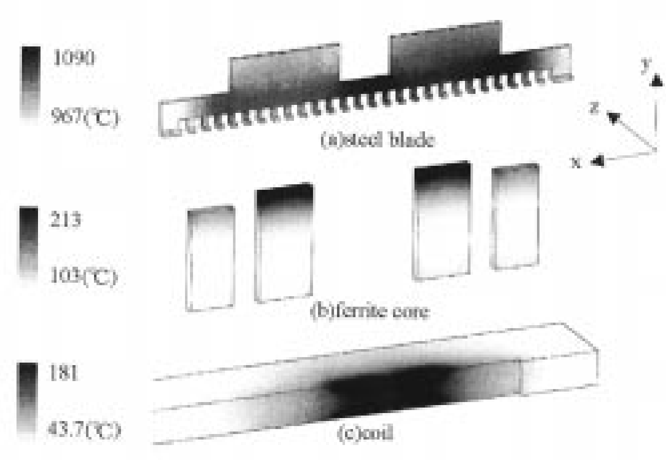

Fig. 3. Temperature distributions in steady state.

in this figure by taking the nonlinearity of the electric conductivity into account.

Fig. 3 shows the temperature distribution of each part in steady state. This figure clearly shows that the temperature near the center of the blade is about 100°C higher than that around both edges. Table II shows the discretization data and CPU time.

B. Influences of Cores for Magnetic Flux Concentration

Fig. 4 shows the distributions of the magnetic flux density vector around steel blades of which models are with and without ferrite cores at the phase angle of 90 degree. It is found that the magnetic flux density of the model with cores (basic model) is greatly higher than that of the model without cores (simple model), but the temperature distribution of the basic model is not uniform in the blade compared with the simple model because of the magnetic flux concentration. Figs. 5 and 6 show the distributions of eddy current density vector of both models. As shown, the eddy current density of the basic model is also

TABLE II
DISCRETIZATION DATA AND CPU-TIME

	Eddy current analysis	Heat Analysis
Number of elements	492,807	
Number of nodes	85,600	
Number of edges	585,224	
Number of unknowns	580,559	85,600
Number of non-zero entries	5,596,229	670,824
CPU time(hours)	24.56	0.69

Computer Used: Sun Microsystems Ultra 1 Model 170

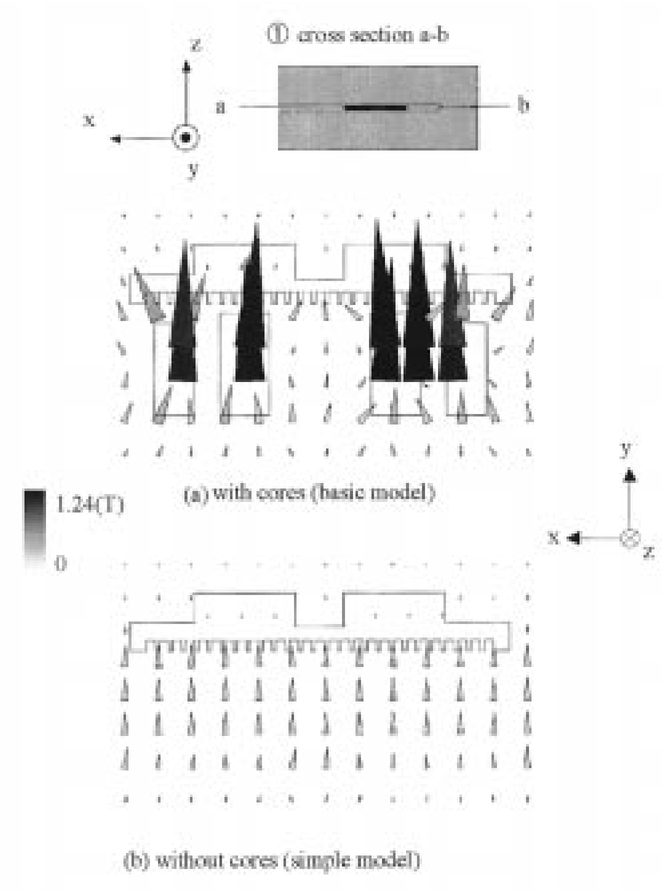

Fig. 4. Distributions of magnetic flux density vectors.

greater than that of the simple model because the eddy current density is proportional to the magnetic flux density. It is found from Fig. 6 that the eddy current concentrates in the blade above four ferrite cores. Fig. 7 shows the temperature distribution of steel blade of the simple model in steady state. Fig. 8 shows the temperature characteristics of the basic model compared with the simple model. As shown, the temperature of basic model is about 400°C higher than that of the simple model. In both models, the temperature near the center of the blade is comparatively higher than that around edges.

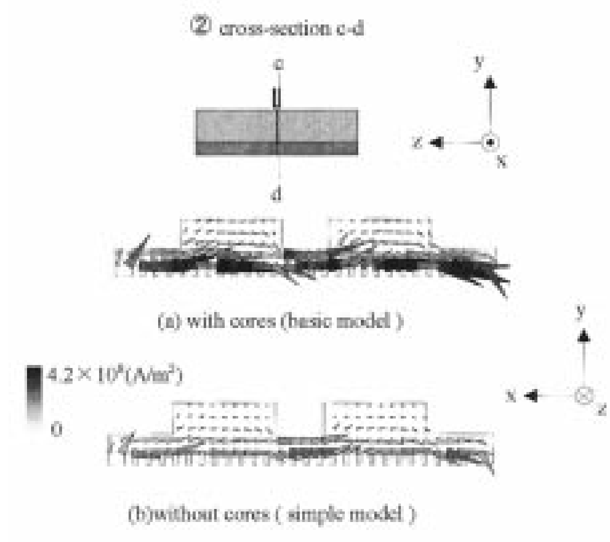

Fig. 5. Distributions of eddy current density vectors.

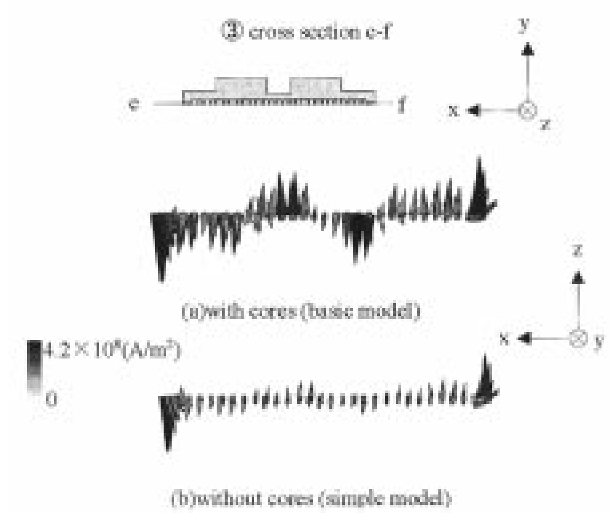

Fig. 6. Distributions of eddy current density vectors.

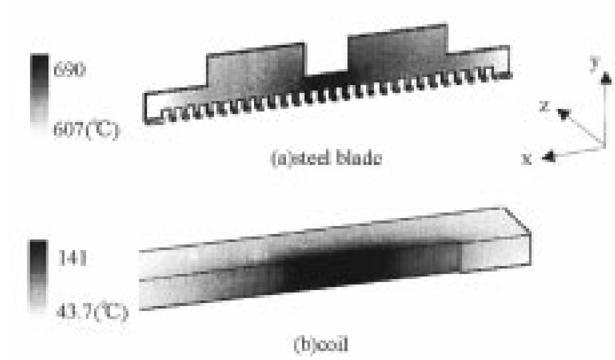

Fig. 7. Temperature distributions of simple model in steady state.

C. Influences of Coil Shape

Figs. 9, 10 and 11 show the distributions of magnetic flux density vector and eddy current density vector around the steel

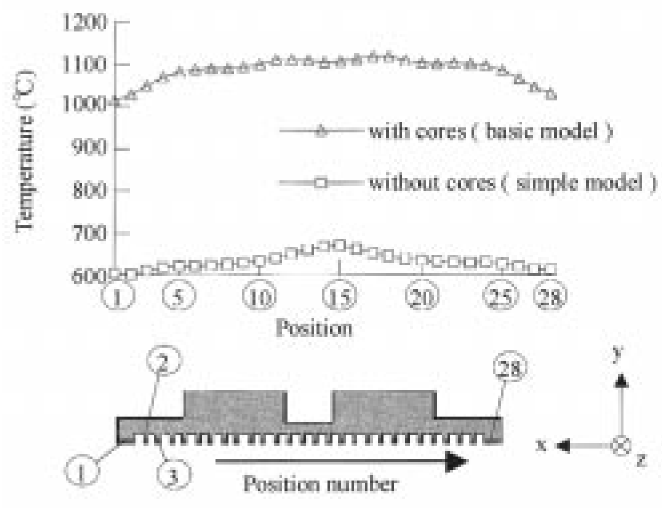

Fig. 8. Influence of cores on temperature.

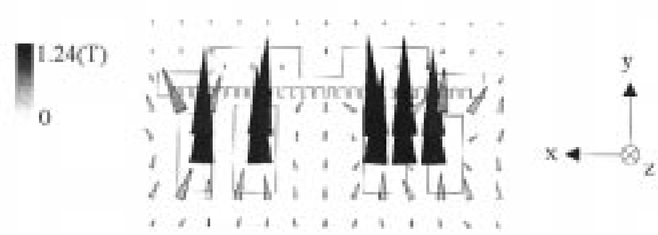

Fig. 9. Distribution of magnetic flux density vectors.

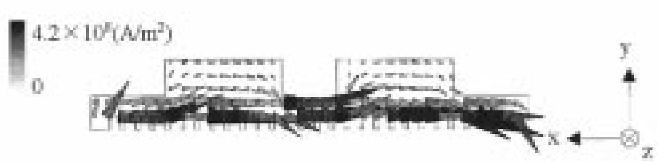

Fig. 10. Distribution of eddy current density vectors.

Fig. 11. Distribution of eddy current density vectors.

blade at the phase angle of 90 degree when the neighborhood of center of the coil is shaved round. It is found that there are not so much differences in these distributions of the steel blade compared with the basic model whether their coils are shaved or not. Fig. 12 shows the temperature distribution of each part in steady state. Fig. 13 shows the comparison of temperature characteristics between the basic model and the coil shaved model. As seen in this figure, the maximum temperature of the coil shaved model is higher than that of the basic model, but the minimum temperature of the former greatly drops compared with the latter.

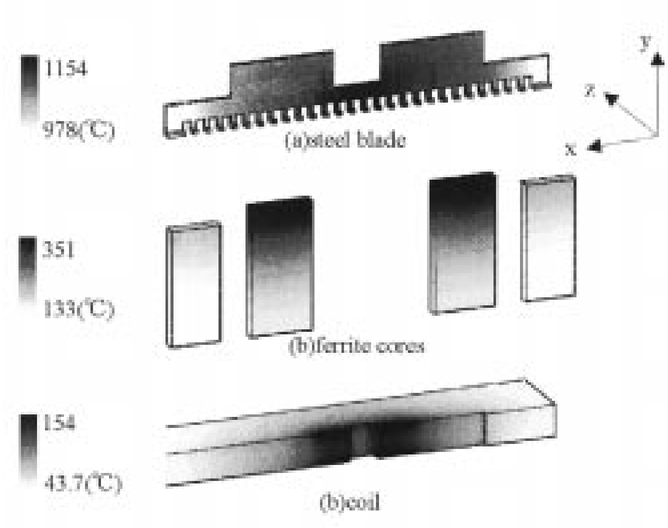

Fig. 12. Temperature distributions of coil shaved model in steady state.

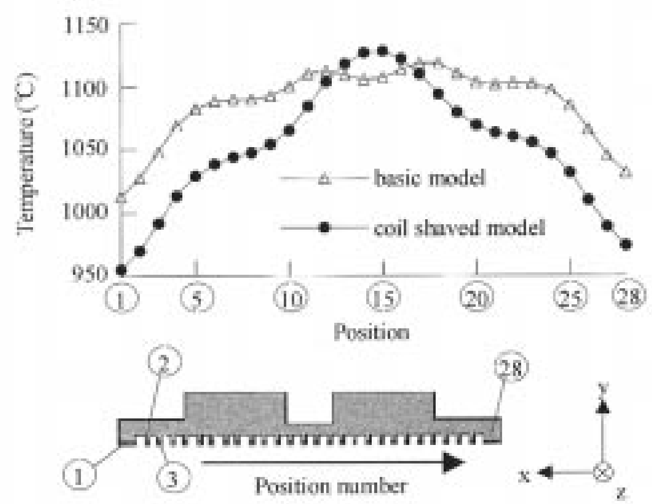

Fig. 13. Influence of coil shape on temperature.

V. Conclusions

This paper introduced a computational method for predicting the temperature characteristics of steel quenching by induction heating. This method was applied to the steel blade quenching of an electric shaver. As the result of that, the computed results had a good agreement with the measured ones by taking the nonlinearity of the electric conductivity into account. Furthermore, the influences of the ferrite cores and the coil shape on the magnetic flux, eddy current and temperature distributions of the steel blade were clarified.

References

[1] K. Hirata, T. Mori, and Y. Kawase, "Thermal analysis of PTC applied resin heater using finite element method," *IEEE Trans. on Magn.*, vol. 35, no. 3, pp. 1654–1657, 1999.

[2] Y. Kawase, H. Mori, and S. Ito, "3-D finite element analysis of electrodynamic repulsion forces in stationary electric contacts taking into account asymmetric shape (Invited)," *IEEE Trans. on Magn.*, vol. 33, no. 2, pp. 1994–1999, 1997.

[3] Y. Kawase, T. Mori, K. Hirata, and Y. Mitsutake, "Performance analysis of electromagnetic ID transmission system using 3-D finite element method," *IEEE Trans. on Magn.*, vol. 34, no. 2, pp. 1994–1999, 1998.